Final report

Estimation of the age/maturity of beef and sheep using spatially resolved visible-near-infrared spectroscopy

Project code: L.EQT.1905

Prepared by: Drs Suresh Thennadil, Mario Palendeng, Tharcilla Alvarenga, and David Hopkins
Charles Darwin University & NSW Department of Primary Industries

Date published: 21 January 2022

PUBLISHED BY
Meat & Livestock Australia Limited
PO Box 1961
NORTH SYDNEY NSW 2059

Meat & Livestock Australia acknowledges the matching funds provided by the Australian Government to support the research and development detailed in this publication.

Abstract

Studies investigating the feasibility of using visible-near-infrared spectroscopy (Vis-NIR) for estimating the age of cattle and sheep and prediction of shear force, collagen content from cattle muscle tissue (*longissimus* and *semitendinosus*), and an investigation of meat-eating quality using spatially resolved diffuse reflectance spectroscopy measurements are covered in this report.

A total of 173 Angus cattle with accurate birth dates were sampled from four different kills. 80 cows were sampled in phase 1 over three kills (LEQT.1626) and 93 cows were sampled in one single kill in phase 2 which was the following study. Vis-NIR scans were collected from hide removed from the neck and loin regions of these animals using a spatially resolved diffuse reflectance fibre optic spectrometer. *Semitendinosus* (eye round) and *Longissimus lumborum* (striploin) muscles were collected from these animals at 1-day post mortem (pm) for subsequent spectral and meat quality analysis. Scans of these samples were collected at 2 days pm. Shear force and collagen content were also determined for these muscle samples.

Vis-NIR scans were also collected from 209 live sheep from Cowra Agricultural Research and Advisory Station – NSW Department of Primary Industries research station ranging from 3 months up to 7 years old. Vis-NIRS scans were collected on the neck and loin region from animals with accurate birth dates. These scans were collected over approximately 8 months. In addition, repetitive measurements over time were collected from 50 sheep at approximately 3, 6, 9 and 12 months of age.

A dual validation approach was used to build and validate partial least squares (PLS) calibration models for estimating age and other parameters considered in this study. This consisted of using the repeated learning and testing (RLT) method and an independent test set randomly chosen from the collected data.

One aspect of this study had the objective of validating the initial results of phase 1 study which was focussed on estimating the chronological age of cattle using VIS-NIR spectroscopy measurements of hide. That study was limited by the distribution of age in the cows. Therefore, in phase 2, data was collected from an additional 93 cows so that a substantial dataset with a good distribution of samples over the age range of interest was available for testing the feasibility of estimating age of cattle using Vis-NIR spectroscopy. Significant challenges were encountered in collecting a suitable dataset that covered a sufficiently evenly distributed cattle age over the age range of interest. As a result of this and considering the time gap between phase 1 and phase 2 studies, the entire data collection was spread over 2 years. As a result, systematic differences between datasets collected from phase 1 and phase 2 was observed which had an adverse effect on model performance.

A standardisation procedure using the finite impulse response (FIR) filter was used to correct the systematic variations arising from changes in instrument characteristics over time. However, this method was not effective in removing these variations and had a limited impact in decreasing the prediction error with the best model that could be produced having an RMSEP of 2.71 years and R^2 of 0.4. The results, while indicating a weak relationship of hide spectra with cattle age, are not sufficient in terms of its usefulness in practice unless the degradation in model performance due to systematic instrument variation can be removed. In order to overcome this, future studies would have to ensure a much shorter data collection period for acquiring the training set to develop the models and should include a rigorous instrument standardisation protocol in order to reduce the impact of changes in the device characteristics over time. Our later experience with devising the experimental protocol and collecting spectra from live sheep, indicates that using live animals will be less complicated than collecting spectra of hides at the abattoir after the slaughter of animals.

It was found that the Vis-NIR measurements, in the wavelength range considered in this research, soluble collagen content can be predicted using spectra from eye round with the best model having an RMSEP of 1.46% and R^2 of 0.41. However, shear force could not be predicted from scans of eye round or from striploin muscles.

The study indicates that the age of sheep can be estimated using spectra collected from the loin and neck region of live animals (Loin: Ring 1, RMSEP = 1.15 years, R^2 = 0.68; Neck: Ring 1, RMSEP = 1.18, R^2 = 0.68). While there was no distinct difference in performance of models based on the sampling region, the model based on spectra from the neck appeared to be less sensitive to age beyond about 3 years. This flattening is also seen to some extent when spectra from the loin region collected by the optical fibres at the shortest source-detector distance and at the two longest source-detector distances.

The stability of the calibration models for predicting the age of sheep was studied by collecting spectra from a batch of 50 sheep when they were 3, 6, 9 and 12 months old. It was found that there was a slight degradation in model performance compared to the initial estimates of prediction error (At 12 months Loin: Ring 1, RMSEP = 1.32 years, Neck: Ring 1, RMSEP = 1.21). As in the case for the cattle data, changes in device characteristics due to drift, parts replacement or misalignment, will affect the long-term usability of the calibration models. Therefore, an instrument recalibration and standardisation protocol has to be developed and applied to the instrument prior to data collection.

An investigation of meat-eating quality based on spatially resolved diffuse reflectance spectroscopy measurement was conducted using spectra from 50 samples of loins, knuckles, and topsides from the same animals. The prediction models were developed with spectra from muscle and the Meat Standard Australia (MSA) score from consumers. Overall, spectra from topside and loin cuts show higher correlations with tenderness scores from consumers compared to the knuckle cut. The highest R^2 value for predicting tenderness and flavour liking was for the topside where the R^2 for tenderness was R^2 = 0.66, RMSEP = 16 and for flavour liking was R^2 = 0.37, RMSEP = 9.42. The highest R^2 value for predicting juiciness was from the model based on loin spectra (R^2 = 0.74, RMSEP = 14.98). In all cases the precision of the predictions was large suggesting the need for a much larger database before the applicability of the models could be established.

Executive summary

Background

This project is a continuation (Phase 2) of LEQT.1626. The main aim of the project was to investigate whether spectra spanning the visible-near-infrared wavelength range of 380 – 1000 nm and collected using a spatially resolved diffuse reflectance set-up, could be used to estimate the age/maturity of slaughter animals with focus on beef cattle and sheep. In addition, the potential to predict shear force, collagen content from cattle muscle tissue (longissimus and semitendinosus), and meat-eating quality using this set-up was also investigated.

Age is a critical factor in determining the market suitability of carcases and eating quality within the Meat Standards Australia (MSA) grading system. The impact of age arises due to the relationships between animal age and maturity, collagen structure and tenderness. Consequently, demarcation occurs after 30 months with older carcases attracting discounts, yet considerable debate still remains on the best way to determine "age". Despite cattle processors assessing the changes of cartilage along the spine by 'ossification', as an additional tool to determine physiological age, estimates can vary with nutrition and health stress. Consequently, an inexpensive, accurate and standardised measure of age could be utilised by industry to facilitate better identification of the true chronological and physiological age of animals. Meat eating quality based on customer experience is dependent on multiple factors such as juiciness, tenderness and flavour. Thus, if the collected spectra can predict meat eating quality, it would provide a cheap and fast prediction of customer experience and thus could inform pricing of the meat.

Objectives

1. Collect spatially resolved diffuse reflectance measurements from sufficient number of cattle and sheep so that data from a wide distribution in age of the animals is achieved. In the case of cattle, the data will be collected from the hide of slaughtered animals. For sheep, the data will be collected from live animals.
2. Develop and evaluate partial least squares regression models for predicting the age of cattle and sheep. In the case of cattle, the additional data collected in this study will be combined to obtain the required distribution of age to validate the results obtained in Phase 1 with the limited data.
3. Perform an evaluation of spatially resolved Vis-NIRS to quantify textural characteristics (tenderness) of meat.
4. Perform an investigation of meat-eating quality using spatially resolved diffuse reflectance spectroscopy measurements.

Methodology

A total of 173 Angus cattle with accurate birth dates were sampled from four different kills. 80 cows were sampled in phase 1 over three kills (LEQT.1626) and 93 cows were sampled in one single kill in phase 2 (this study). Vis-NIR scans were collected from hide removed from the neck and loin regions of these animals using a spatially resolved diffuse reflectance fibre optic spectrometer. *Semitendinosus* (eye round) and *Longissimus lumborum* (striploin) muscles were collected from these animals at 1-day post mortem (pm) for subsequent spectral and meat quality analysis. Scans of these samples were collected at 2 days pm. Shear force and collagen content were also determined for these muscle samples.

In the case of sheep, Vis-NIR scans were collected from live animals. Scans were taken from 209 live sheep from Cowra Agricultural Research and Advisory Station – NSW Department of Primary

Industries research station ranging from 3 months up to 7 years old. Vis-NIRS scans were collected on the neck and loin region from animals with accurate birth dates. These scans were collected over approximately 8 months. In addition, repetitive measurements over time were collected from 50 sheep at approximately 3, 6, 9 and 12 months of age.

A dual validation approach was used to build and validate partial least squares (PLS) calibration models for estimating age and other parameters considered in this study. This consisted of using the repeated learning and testing (RLT) method and an independent test set randomly chosen from the collected data.

Phase 1 study which was focussed on estimating the chronological age of cattle using VIS-NIR spectroscopy measurements of hide. That study was limited by the distribution of age in the cows. Therefore, in phase 2, data was collected from an additional 93 cows so that a substantial dataset with a good distribution of samples over the age range of interest was available for testing the feasibility of estimating age of cattle using Vis-NIR spectroscopy. Significant challenges were encountered in collecting a suitable dataset that covered a sufficiently evenly distributed cattle age over the age range of interest. As a result of this and considering the time gap between phase 1 and phase 2 studies, the entire data collection was spread over 2 years. Systematic differences between datasets collected from phase 1 and phase 2 was observed which had an adverse effect on model performance. A standardisation procedure using the finite impulse response (FIR) filter was used to correct the systematic variations arising from changes in instrument characteristics over time.

Results/key findings

The best model that could be produced for estimating the age of cattle from spectra of hides had a root mean square error of prediction (RMSEP) of 2.71 years and R^2 of 0.4. The results, while indicating a weak relationship of hide spectra with cattle age, are not sufficient in terms of its usefulness in practice unless the degradation in model performance due to systematic instrument variation can be removed. In order to overcome this, future studies would have to ensure a much shorter data collection period for acquiring the training set to develop the models and should include a rigorous instrument standardisation protocol in order to reduce the impact of changes in the device characteristics over time. Furthermore, the complexity of the protocol due to the nature of collecting the hide samples and making it measurement ready, made it difficult to achieve consistently accurate measurements. This could also have contributed to the high prediction errors. Our later experience with devising the experimental protocol and collecting spectra from live sheep, indicates that using live animals will be less complicated than collecting spectra of hides at the abattoir after the slaughter of animals.

It was found that the Vis-NIR measurements in the wavelength range considered in this research cannot be used to predict shear force using spectra collected from either the striploin or eye round muscles with R^2 values less than 0.05 and 0.2 respectively.

Despite the systematic instrument variations affecting the models, the results suggest that soluble collagen content can be predicted using spectra from eye round with the best model having an RMSEP of 1.46% and R^2 of 0.41. On the other hand, spectra from striploin muscles had no relationship with soluble collagen content with the models having an R^2 of less than 0.1.

The study indicates that the age of sheep can be estimated using spectra collected from the loin and neck region of live animals (Loin: Ring 1, RMSEP = 1.15 years, R^2 = 0.68; Neck: Ring 1, RMSEP = 1.18, R^2 = 0.68). While there was no distinct difference in performance of models based on the sampling region, the model based on spectra from the neck appeared to be less sensitive to age beyond about 3 years. This flattening is also seen to some extent when spectra from the loin region collected by the optical fibres at the shortest source-detector distance and at the two longest source-detector distances.

The stability of the calibration models for predicting the age of sheep was studied by collecting spectra from a batch of 50 sheep when they were 3, 6, 9 and 12 months old. It was found that there was a slight degradation in model performance compared to the initial estimates of prediction error (At 12 months Loin: Ring 1, RMSEP = 1.32 years, Neck: Ring 1, RMSEP = 1.21).

An investigation of meat-eating quality based on spatially resolved diffuse reflectance spectroscopy measurement was conducted using spectra from 50 samples of loins, knuckles, and topsides from the same animals. The prediction models were developed with spectra from muscle and the Meat Standard Australia (MSA) score from consumers. Overall, spectra from topside and loin cuts show higher correlations with tenderness scores from consumers compared to the knuckle cut. The highest R^2 value for predicting tenderness and flavour liking was for the topside where the R^2 for tenderness was $R^2 = 0.66$, RMSEP = 16 and for flavour liking was $R^2 = 0.37$, RMSEP = 9.42. The highest R^2 value for predicting juiciness was from the model based on loin spectra ($R^2 = 0.74$, RMSEP = 14.98). In all cases the precision of the predictions was large suggesting the need for a much larger database before the applicability of the models could be established.

Benefits to industry

The results indicate that the Vis-NIR measurements have the potential to provide information regarding cattle age and on other factors affecting meat quality. Such a technology, if fully developed, can be of high value to industry by providing an inexpensive and standardised measure of age and, more broadly, meat quality could inform pricing of the meat.

Future research and recommendations

Three recommendations arise from the study for determining cattle age. Firstly, the collection of calibration dataset should be over a short time span of 2 – 3 months. Secondly, a rigorous protocol for standardising the instrument must be developed for long-term maintenance of the calibration model since the device will be used for a long time and carrying out a full calibration at regular intervals would not be feasible. Thirdly, given the experience during data collection from live sheep, acquiring spectra from live cattle instead of hides at slaughter will be preferable.

The results suggest that meat eating quality traits can be predicted with limited ability using spectroscopy in the wavelength range of 850-990nm. The large uncertainty in the predictions could be addressed by collecting a much larger dataset.

Prediction of age using spectra taken from live sheep shows promise. The flattening of the prediction at higher age values may be overcome using nonlinear approaches. Thus, future studies should focus on collecting a larger dataset so that nonlinear methods. Additionally, as in the case of cattle, it is recommended that rigorous standardisation approaches need to be developed for long-term maintenance of the calibration model.

Table of contents

Abstract 2
Executive summary 4
1. Background 8
2. Objectives 9
3. Methodology 9
3.1 Data Collection 9
3.1.1 Animal Background 9
3.1.2 Abattoir Data Collection - Beef 10
3.1.3 Meat Sampling - Beef 10
3.1.4 Live Sheep Scans 10
3.1.5 Meat-Eating Quality Data 11
3.1.6 Instrument Configuration 11
3.2 Data Processing, Modelling and Validation 12
3.2.1 Standardisation using FIR filter method 12
3.2.2 Training and Model Validation 13
4. Results and Discussion 16
4.1 Prediction of Chronological Age of Cattle 16
4.1.1 Prediction of age using spectra collected from muscles 18
4.2 Prediction of Chronological Age of Cattle 19
4.2.1 Prediction of age using spectra collected from muscles 19
4.2.2 Soluble collagen prediction using spectra collected from muscles 20
4.3 Prediction of Chronological Age Using VIS-NIR scans of live sheep 21
4.3.1 Stability of calibration models 24
4.4 Prediction of Meat Eating Quality 26
4.4.1 Prediction of meat eating quality using spectra of loin muscles 26
4.4.2 Prediction of meat eating quality using spectra of topside muscles 29
4.4.3 Prediction of meat eating quality using spectra of knuckle muscles 31
5. Conclusion 33
6. Acknowledgements 34
7. References 35

1. Background

This project is a continuation (Phase 2) of the project LEQT.1626. While the background and motivation for the research was described in that report, they are revisited here for the purpose of completeness and for making this report self-contained.

Animal age is a critical factor in determining the market suitability of carcases and eating quality (Duarte et al., 2011; Schönfeldt et al., 2011). The impact of age arises due to the relationships between animal age and maturity, collagen structure and tenderness. Consequently, demarcation occurs after 30 months with older carcases attracting discounts, yet considerable debate still remains on the best way to determine "age". In sheep, teeth eruption is used for estimating age which is known to be weakly related to the chronological age (Hopkins et al., 2007). In beef, dentition and/or ossification are used. In this regard, ossification is currently the "gold standard" to estimate the maturity of animals. This evaluation requires trained graders and as such is subjective and therefore susceptible to uncertainties and errors dependant on the grader. In addition, commercial beef cattle are mostly slaughtered around 18 to 30 months of age and at this stage the animal may have 0, 2, 4 or 6 permanent incisors. This inconsistency causes penalties in the carcase price up to 7.5%.

Cattle processors assess the changes of cartilage along the spine by 'ossification', as an additional tool to determine physiological age. However, these estimates can vary significantly as ossification is affected by several factors such as nutrition, growth path, gender, genetics, hormone status and animal health. The ossification score of heifers has been observed to be15 % higher than steers, and cattle implanted with hormonal growth promotants (HGPs) have a 10% higher bone ossification (Cafe et al., 2010).

In addition, dentition and ossification score show disagreement in the maturity and age classification of young cattle, which is not suitable for an industry wanting to accurately predict the eating quality of meat. Lawrence et al. (2001) compared the US Department of Agriculture (USDA) ossification system with dentition system and showed that over 9 % of the steers were classified as maturity B (30-42 months old) but had 0 permanent incisors (typically < 18 months old). In sheep, there is no method being used to estimate maturity of the animal in the abattoir and only dentition is used to estimate age.

The highest ossification score is 590 in the Meat Standards Australia (MSA) maturity system which is usually reached when the animal is 5 to 6 years old, yet animals are slaughtered for meat at ages up to 14 years old. Hence, cattle between 6 and 14 years of age cannot be differentiated in age or physiological maturity, and thus are classified and sold as the same even though data shows the eating quality of these animals is different (Bonny et al 2016).

Consequently, an inexpensive, accurate and standardised measure of age could be utilised by industry to facilitate better identification of the true chronological and physiological age of animals and which provides the ability to estimate ages beyond 5-6 years.

Work in beef has shown that the weight of the eye lens is strongly related to true age (Raines et al., 2008), but the practicalities of adopting this measure prevent application. The use of spectroscopic technology can effectively provide information on the structure of tissues, as affected by age. Work on human's shows that it is possible to determine the age of people using NIRS scans of skin (Ruchti et al. US Patent, 2002). In principle, this should translate to animals. Interestingly, regarding the NIRS evaluation of the skin of slaughter animals, one study has shown NIRS of the ear skin can be a fast method to classify pork carcases on fatness and fatty acid composition (Prieto et al., 2015). The results from Phase 1 of the project showed the potential of this approach (LEQT.1626; Palendeng et al, 2020)

This project examines whether visible-near-Infrared (Vis-NIR) spectra of skin/hide samples of cattle and sheep can be used to accurately estimate their age/maturity. Conceptually, a small area of skin and muscle will be evaluated (either on live animals or from hide samples) on line and at line speed, attempting to provide an accurate estimate of animal age/maturity and its effect on eating quality.

Meat eating quality based on customer experience is dependent on multiple factors such as juiciness, tenderness and flavour. Thus, if the collected spectra can predict meat eating quality, it would provide a cheap and fast prediction of customer experience and thus could inform pricing of the meat.

Spatially resolved spectroscopy (SRS) measurements instead of standard reflectance spectroscopy measurements were used in this study. SRS consists of using fibre-optic probes which delivers light through a fibre and collects reflected light. The reflected light is sourced from different distances from the source fibre using detection fibres placed at different distances from the source fibre (Hjalmarsson and Thennadil, 2008). Thus, it provides reflected signals which have traversed different paths and distances within the tissue sample. Such as set up will provide the means to find the optimal source-detector distance in terms of calibration model performance.

2. Objectives

1. Collect spatially resolved diffuse reflectance measurements from sufficient number of cattle and sheep so that data from a wide distribution in age of the animals is achieved. In the case of cattle, the data will be collected from the hide of slaughtered animals. For sheep, the data will be collected from live animals.
2. Develop and evaluate partial least squares regression models for predicting the age of cattle and sheep. In the case of cattle, the additional data collected in this study will be combined to obtain the required distribution of age to validate the results obtained in Phase 1 with the limited data.
3. Perform an evaluation of spatially resolved Vis-NIRS to quantify textural characteristics (tenderness) of meat.
4. Perform an investigation of meat-eating quality using spatially resolved diffuse reflectance spectroscopy measurements.

3. Methodology

3.1 Data Collection

3.1.1 Animal Background

A total of 173 Angus Cull cows with accurate birth dates were sampled from four different kills. 80 cows were sampled in phase 1 over three kills (LEQT.1626) and 93 cows were sampled in a single kill in phase 2 (L.EQT.1905), which was the subsequent study.

Kill 1 and kill 2 took place around 2 months apart and kill 2 and kill 3 around 8 days. Kill 3 (phase 1) and kill 4 (phase 2) were apart by approximately 1.5 years. Thus, the entire data collection was spread over nearly 2 years.
Visible – Near Infrared (Vis-NIR) scans were also collected from 209 live sheep from Cowra Agricultural Research and Advisory Station – NSW Department of Primary Industries research

station – with well recorded birth dates and ranging from 3 months up to 7 years old. The scans were collected over approximately 8 months. In addition, repetitive measurements over time were collected from 50 animals at approximately 3, 6, 9 and 12 months of age from September 2019 to June 2020.

3.1.2 Abattoir Data Collection - Beef

At slaughter EID and RFID were electronically recorded along with carcase body number in order to match animal background ID with carcase information. Dentition was assessed at slaughter based on the number of permanent incisors in a classification from 0 (milk teeth) to 8 (full mouth). Dentition ranged from 4 to 8 with the majority of the cows scored at 8. Ossification score was visually assessed in the chiller using the scale developed by United States Department of Agriculture grading service that runs from 100 to 590 in 10-point increments.

Entire hides were collected with animal ID attached. Whole hides were individually placed on a table, clipped and a sub-sample of approximately 10 x 10 cm was collected on the neck and loin region. The samples were labelled and bagged for subsequent spectral analysis. Prior to the spectral scans the hides were shaved using a safety razor, placed on a block of meat and then scanned using a spatially resolved spectroscopy system.

While the scans from 173 cows were collected, 5 scans were discarded from kill 4 due to the abnormal spectral intensity of the collected scans. Therefore, only 168 samples were included in the analysis.

3.1.3 Meat Sampling - Beef

*Semitendinosu*s (eye round – H.A.M. No. 2040*) and *Longissimus lumborum* (striploin – H.A.M. No. 2140*) muscles were collected at 1-day post mortem (pm) from the left side of the carcase for subsequent spectral assessment, tenderness and connective tissue analysis.

Primal cuts were transported in eskies with ice from the abattoir to the meat laboratory. At 2 days pm both muscles (eye round and striploin) were sub-sampled in the chiller at 4 °C for spectra scans at 2 days pm. A meat block (~200 g) was sectioned for shear force analysis and a 50 ml tube filled with diced meat for collagen analysis were frozen at -20 °C for subsequent assessment.

3.1.4 Live Sheep Scans

Visible – Near Infrared (Vis-NIR) scans were collected from 209 live sheep at 2 different locations on the animals (neck and loin) using the SRS-NIRS device (same instrument used in the beef study). The measurement spots on the animals were shaved prior to acquiring the scans. Due to data collection error, 1 sheep scan collected from the loin region and 2 from the neck were discarded leaving 208 sheep scans from the loin and 207 samples from the neck suitable for analysis.

A group of 50 animals chosen from the 209 sheep, which were scanned at 3, 6, 9 and 12 months of age. It was expected that an additional investigation on live animals for age prediction based on scans of the same animal through life could provide additional insights into the stability of the prediction over time.

* *H.A.M. - Handbook of Australian Meat Reference Cut Item and Code Number*

3.1.5 Meat-Eating Quality Data

A total of 50 lamb samples from Merino lambs approximately 11 months old were collected as part of the "L.EQT.1908 Eating quality in Merino breeding programs" project. Samples were collected to investigate the potential of using Vis-NIR SRS to determine the eating quality of lamb. At 1 day *post mortem* loin (*longissimus lumborum*), knuckle (*quadriceps femoris*) and topside (*semimembranosus*) muscles were collected and scans using the spatially resolved diffuse reflectance Vis-NIR spectroscopy obtained. Primal cuts were vacuum packed and transported in portable cooling boxes with ice from the abattoir to the meat laboratory. At 5 days pm the muscles were sub-sampled for sensory analysis and frozen at -20 °C.

Sensory analysis was conducted based on the MSA meat eating quality protocols. Each individual muscle was sliced into 10 samples, thus the average of 10 consumer responses were used in the analysis of each sensory parameter. Consumers were recruited from the community to represent diverse backgrounds, areas and age (between 18 and 70 years old). Meat samples were grilled and seven different samples were served per consumer. Each consumer completed a score sheet for every sample tested using a score from 0 to 100, this involved marking lines to score tenderness, juiciness, liking of flavour and overall liking (MSA beef information kit, 2018).

3.1.6 Instrument Configuration

The SRS device is the same one as that used for the phase 1 study. The probe consists of a source fibre, which delivers light to the sample and 5 concentric rings of detection fibres to collect light reflected from the sample. Each ring consists of 4 detection fibres as illustrated in Fig. 1. The light collected by different rings of fibres travels different distances within the sample and thus has potentially different levels of information. The probe chosen for the study consisted of rings of fibres placed at centre-to-centre distances of 0.5, 1.0, 1.5, 2.0, and 2.5 mm from the source fibre respectively. These will be referred to as ring 1 …. ring 5 respectively in this report. Further details can be found in the phase 1 final report (Thennadil et al., 2019).

Figure 1. Source and detector fibre configuration in Probe #1. Fibre in the centre is the 400 µm diameter source fibre. The surrounding fibres are the 200 µm detection fibres

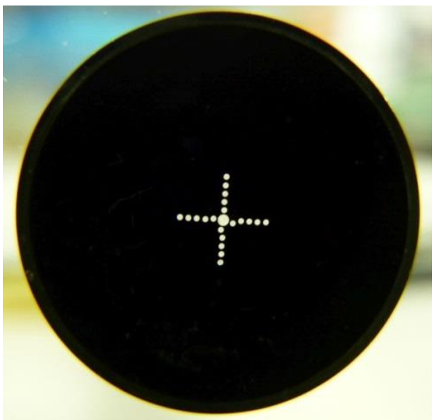

3.2 Data Processing, Modelling and Validation

3.2.1 Standardisation using FIR filter method

As indicated earlier, the spectral data collection spanned nearly two years over 4 kills. This was due to difficulty in accessing cows spanning a wide age range and with an accurate record of birth dates. In addition, there was a long gap between the end of phase 1 and the beginning of phase 2, resulting in a gap of 1.5 years between kills 3 and 4. As a result, systematic differences between datasets collected from phase 1 and phase 2 were observed. Fig. 2 shows the mean and standard deviations of spectra collected from the neck region using ring 1. It can be seen that the intensity from phase 2 is slightly lower compared to the data from phase 1. Spectra collected from kills 3 and 4, which were only 8 days apart lie closest to each other. Similar variations were also seen in measurements from rings 2 to 5. Variation in spectra intensity could be due to instrument drift, ambient temperature changes during data collection, and any changes or adjustments to the instrument such as replacement of lamp etc (Fern, 2001; Bouveresse & Massart, 1996; Adamovsky et al., 1990; Salim et al., 2011; Mark & Workman, 2017). Under these circumstances, simple normalisation and pre-processing methods do not adequately remove these effects and standardisation techniques have to be applied to the dataset.

Figure 2. The mean and standard deviation of spectra from Kills 1 – 4 collected from the neck location using ring 1

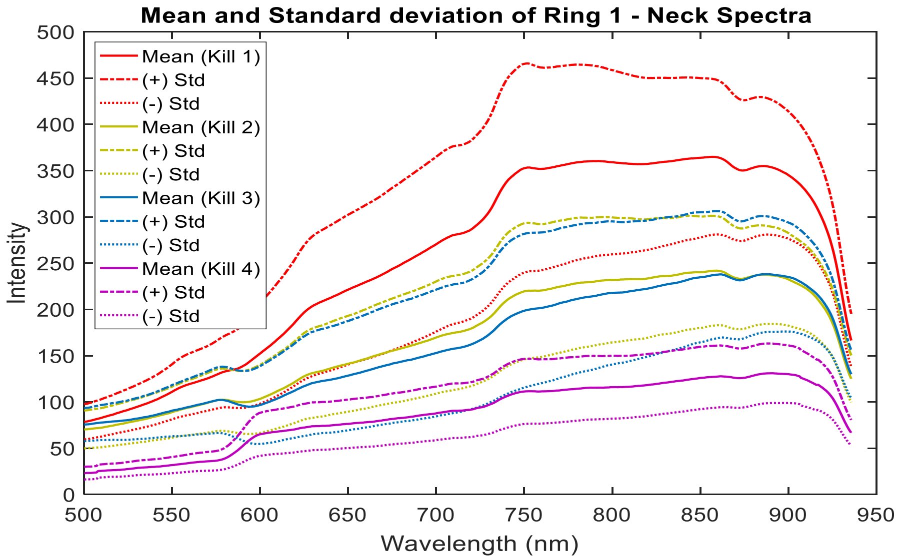

The Finite Impulse Response (FIR) filter (Fern, 2001) method was chosen as it does not require reference spectra which closely resemble the sample spectra. The FIR filter requires one target spectrum for the standardisation. The mean of Kill 2 spectra was used as the target spectrum as the spectra from this kill overlaps with spectra from the other kills. Fig. 3 shows the data before and after the application of the FIR filter.

Figure 3. Standardisation using FIR filter. Spectra of all kills (a) before and (b) after applying the FIR filter

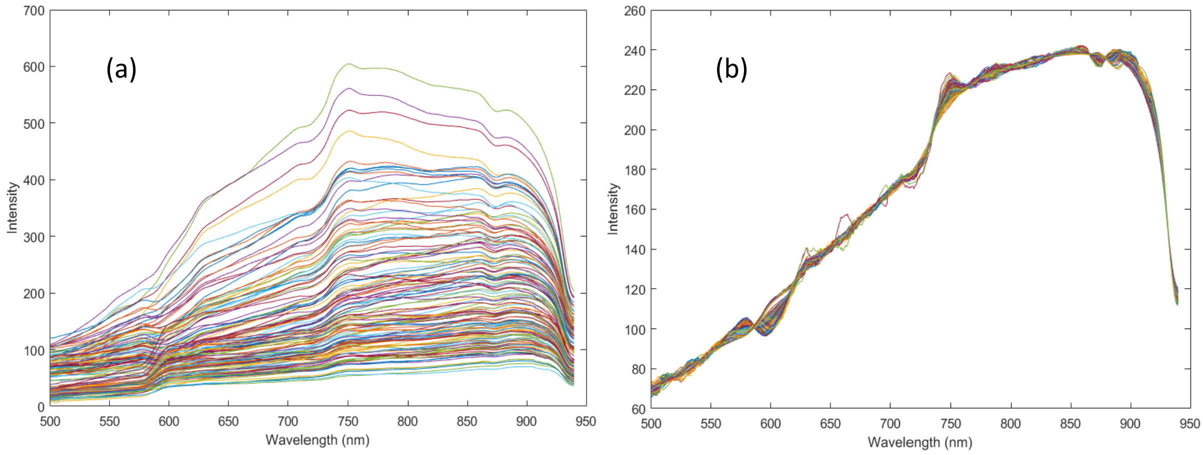

It can be seen that the spectra “collapse” into a narrow band of values with the bulk of the variance in the original data set being removed. Visually, it appears that the effect of the kill date is removed by the standardisation process. However, a deeper look into the standardised dataset indicated that this was not the case. Principal component analysis (PCA) was conducted on the dataset before and after the application of the FIR standardisation. As can be seen from Fig. 4, the kill 4 spectra are distinctly separate compared to the other 3 kills even after standardising the spectra using the FIR filter. This could have a significant impact on the calibration model performance which will be discussed later in this report.

Figure 4. PCA of spectra (a) before and (b) after applying the FIR filter

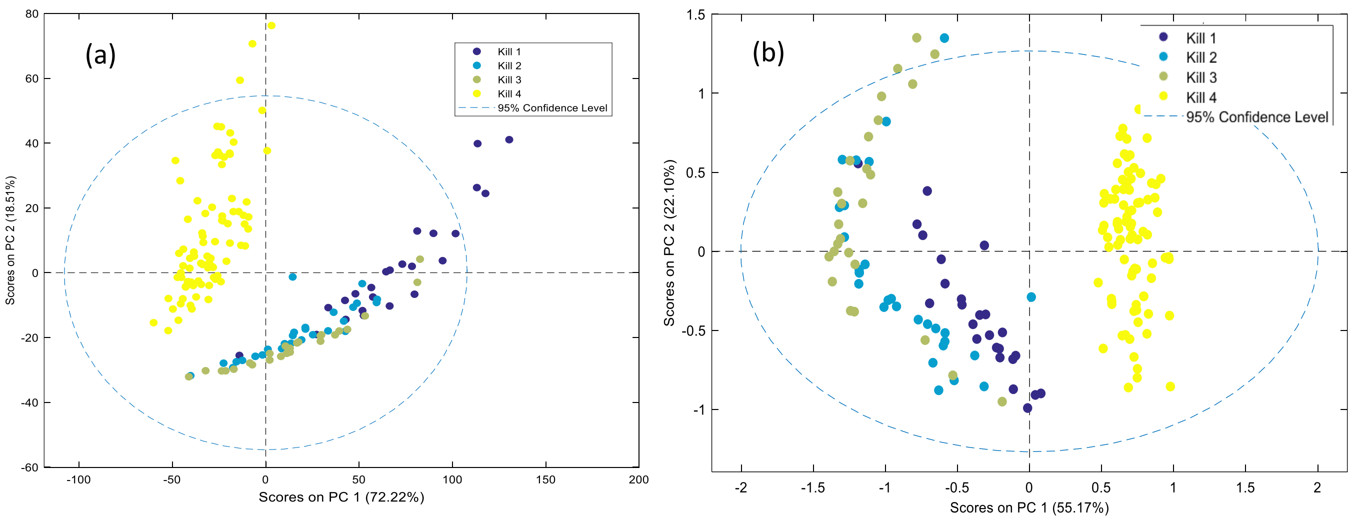

3.2.2 Training and Model Validation

In phase 1, a simple leave-one-out cross-validation scheme was used due to the small dataset and the lack of sufficient data spanning the desired age range. As indicated in the phase 1 report, the leave-one-out cross-validation tended to give optimistic estimates of model performance. With the larger dataset, we have used a more rigorous approach to evaluate model performance.

Fig. 5 provides a flowchart illustrating the training-validation approach used to evaluate the models built for estimating age and other properties considered in this study. The dataset was divided randomly into a training and validation set. The training set was used to build models. Validation was done at two levels. The first was as part of the repeated learning and testing (RLT) method which was used to obtain a robust estimate of the optimum number of latent variables, carry out wavelength selection and finally build the final model which was applied to the "unseen" validation set. Since, dividing the data once into training and validation set could lead to conclusions which are biased by the division of the dataset due to the finiteness of the validation set, the validation through repeated RLT provides an additional metric in the form of an average root mean square error of prediction (ARMSEP). If the value of ARMSEP is consistent with the root mean square error of prediction based on the unseen validation dataset, it would provide greater confidence in the evaluation of model performance. The RLT method is essentially the repeated application of training and validation by randomly splitting the training dataset into an independent training (calibration) and test set.

The algorithm includes the application of a genetic algorithm for wavelength selection. The inner loop of K-folds cross validation (box with red dashed line) is used to estimate the optimum number of latent variables and to select the optimum set of wavelengths. The RMSEP values obtained from each of the 20 iterations of splitting the dataset and carrying out the training and validation are averaged to obtain the ARMSEP.
For the cattle dataset, the combined dataset consisting of spectra from all the kills was randomly divided into training set consisting of 138 samples and a validation set of 30 samples. In the RLT loop the split between training and test set was 118 and 20 samples respectively. Spectra were pre-processed using the standard normal variate (SNV) method and mean-centred prior to building models.

For building and evaluating calibration models for live sheep, 50 samples were set aside as the unseen validation set. As in the case of the cattle dataset, in the RLT loop, 20 samples were used as a test set. Mean-centred spectra were used for model building.

Model building and analysis were carried out using Matlab (The Mathworks Inc. (2016), MATLAB, 64-bit (win64)) and the PLS Toolbox (Eigenvector Research, 2016).

Figure 5. Implementation of repeated learning (RTL) calibration and validation of models

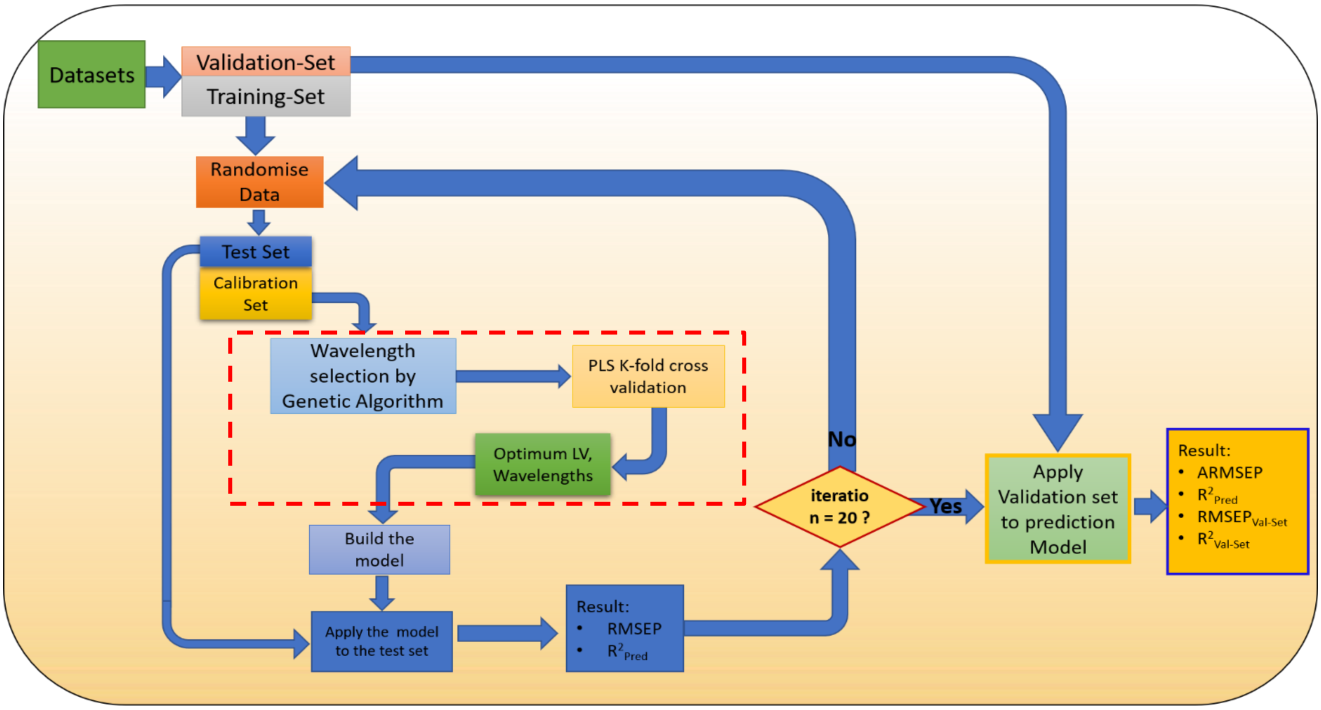

For meat-eating quality prediction, 10 out of the 50 samples were set aside as unseen validation set. For each iteration of the RLT algorithm, the remaining 40 samples were split randomly into calibration (35 samples) and test set (5 samples).

4. Results and Discussion

4.1 Prediction of Chronological Age of Cattle

Table 1 shows the results obtained using the calibration-validation approach applied to hide samples from the neck and loin regions measured using scans from rings 1 to 5. The number of latent variables reported is the one that was chosen as the optimum number of LVs most frequently and the number in the brackets is the number of times it was picked as the optimum number out of the 20 iterations. The uncertainty in the ARMSEP is given as ± standard error of the ARMSEP. This format is followed in all the subsequent tables. The model performance is analysed by considering the consistency between RMSEP (from unseen data) and ARMSEP (from RLT), the R^2 obtained from the unseen data as well as the one obtained from the RLT process and the number of times the optimum number of LVs is chosen (which is an indication of stability of the model with respect to the training set used to build it).

Table 1. Model performance using spectra from neck and loin region without FIR standardisation for predicting age of cattle

	ARMSEP	R^2 Prediction	Optimum no. of LVs (no. of occur)	RMSEP Unseen	R^2 Unseen
Neck – ring 1	3.07 ± 0.06	0.27	4 (17)	2.87	0.34
Neck – ring 2	3.07 ± 0.09	0.29	4 (14)	2.78	0.37
Neck – ring 3	3.09 ± 0.07	0.31	4 (15)	3.05	0.28
Neck – ring 4	2.88 ± 0.08	0.38	4 (15)	2.77	0.38
Neck – ring 5	3.15 ± 0.09	0.27	4 (12)	2.86	0.35
Loin – ring 1	3.12 ± 0.08	0.32	5 (14)	3.33	0.17
Loin – ring 2	2.93 ± 0.06	0.34	4 (14)	2.94	0.31
Loin – ring 3	3.01 ± 0.07	0.37	4 (14)	3.04	0.31
Loin – ring 4	3.05 ± 0.10	0.32	4 (14)	2.80	0.37
Loin – ring 5	3.18 ± 0.08	0.30	5 (14)	2.80	0.37

Figure 6. Scatter plot of the age estimated using a PLS model without standardisation using FIR filter with spectra collected from Neck region by ring 4. RMSEP = 2.77 years and R^2=0.38

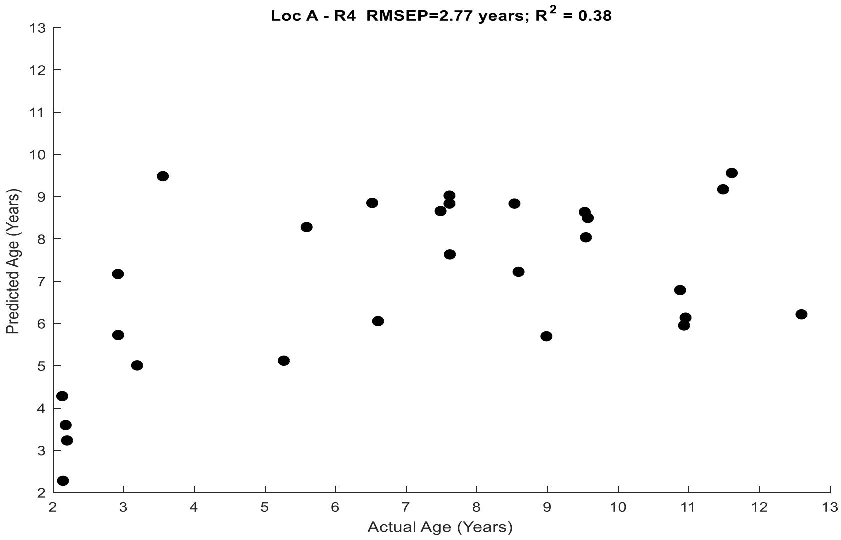

The results indicate that many of the models have a statistically significant though weak relationship with age with best overall models arising from ring 4 measurements of the hide samples from the neck and loin region. As can be seen from Fig. 6, the variance around the predicted age is a result of the low correlation.

Next, we examine the impact of standardising the spectra using the FIR filter. From Table 2, it can be seen that again ring 4 measurements provide the best model performance. Comparing Table 1 and 2, standardisation using FIR provides a slightly better model performance. The scatter plot (Fig. 7) also shows a slight improvement compared to Fig. 6.

The results from Table 1 and 2 show that there is a very little difference between the prediction of age using spectra with and without the FIR filter. This indicates that the FIR filter is not an effective standardisation approach for this dataset. The PCA plots in Fig. 4 indicate that this is due to the FIR filter being unable to satisfactorily remove the systematic differences in the kill 4 spectra with respect to the other three kills as was evidenced in the PCA plots in Fig. 4.

Model performance without wavelength selection being included was also examined. It was found that (results not shown here), the results were not significantly different from the ones where wavelength selection was included.

Table 2. Model performance using spectra from neck and loin region with FIR standardisation for predicting age

	ARMSEP	R^2 Prediction	Optimum no. LVs (no. of occur)	RMSEP Unseen	R^2 Unseen
Neck – ring 1	2.89 ± 0.05	0.31	4 (20)	2.80	0.36
Neck – ring 2	3.01 ± 0.07	0.32	4 (20)	2.80	0.36
Neck – ring 3	2.82 ± 0.07	0.34	4 (19)	2.88	0.35
Neck – ring 4	2.97 ± 0.06	0.34	4 (20)	2.71	0.40
Neck – ring 5	3.08 ± 0.08	0.32	4 (20)	2.76	0.37
Loin – ring 1	2.82 ± 0.08	0.39	5 (9)	3.04	0.25
Loin – ring 2	2.81 ± 0.06	0.41	4 (10)	2.94	0.30
Loin – ring 3	3.07 ± 0.09	0.33	4 (9)	2.80	0.37
Loin – ring 4	2.93 ± 0.07	0.35	4 (17)	2.71	0.40
Loin – ring 5	2.96 ± 0.09	0.33	3 (14)	2.78	0.39

Figure 7. Scatter plot of the age estimated using a PLS model with standardisation using FIR filter with spectra collected from Neck region by ring 4. RMSEP = 2.71 years and R^2=0.40

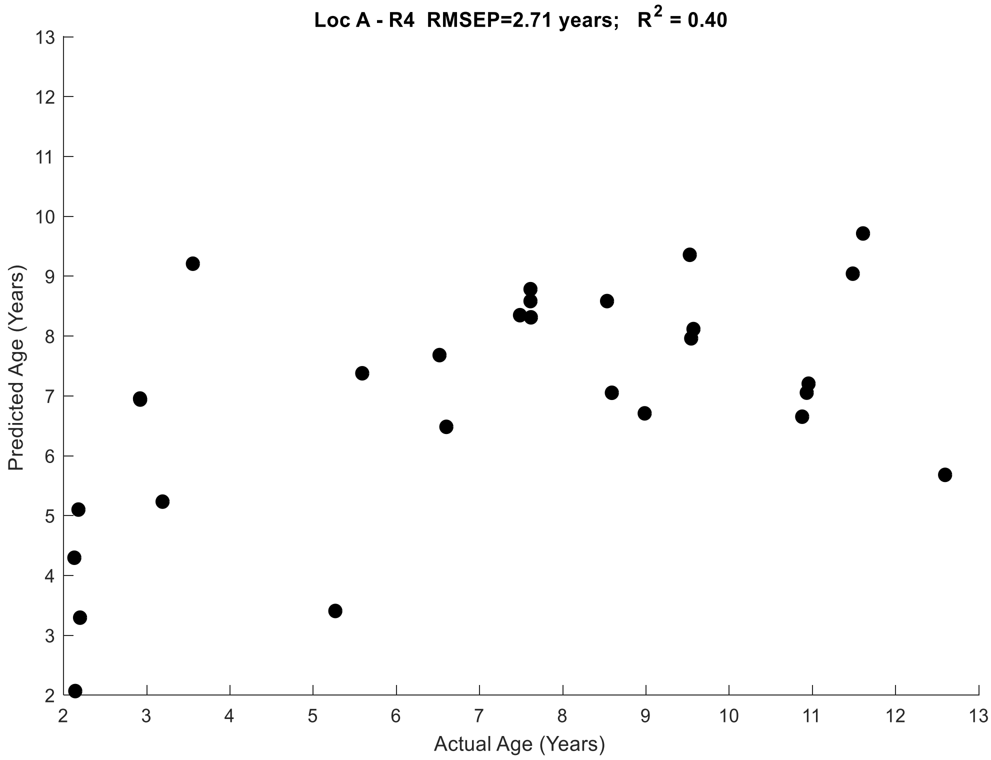

4.1.1 Prediction of age using spectra collected from muscles

Spectra from striploin and eye round muscles collected at 2 days post-mortem were used to develop and assess models for predicting age of cattle. The results presented here are based on models built without including wavelength selection as part of the model building and validation procedure. Wavelength selection was not applied, given the analysis with hide spectra indicated no significant improvement when wavelength selection was applied. Table 3 summarises the results obtained when spectra standardised with the FIR filter were used for building and evaluating models. Based on the unseen validation set, it can be seen from Table 3, that the predictive ability of the models is weak given that the RMSEP on the unseen data set is greater than 3 years even though the ARMSEP from the RLT iterations indicates, on average, a slightly better model performance than that indicated by the unseen dataset. In general, eye round appears to provide a better and more stable model, based on the optimum number of LVs and the number of times they are chosen in the RLT iterations, compared to the striploin muscle.

Table 3. Model performance using spectra from neck and loin region with FIR standardisation for predicting age (SL – Striploin, ER – Eye Round)

Spectra	ARMSEP	R^2 Prediction	Optimum no. of LVs (no. of occur)	RMSEP Unseen	R^2 Unseen
SL - ring 1	2.81 ± 0.07	0.36	3 (11)	3.34	0.24
SL - ring 2	2.70 ± 0.08	0.40	3 (15)	3.41	0.21
SL - ring 3	2.77 ± 0.07	0.38	3 (16)	3.38	0.23
SL - ring 4	2.71 ± 0.07	0.41	5 (18)	3.19	0.31
SL - ring 5	3.02 ± 0.07	0.29	6 (17)	3.11	0.38
ER - ring1	2.70 ± 0.09	0.37	2 (19)	3.13	0.33
ER - ring 2	2.67 ± 0.08	0.38	2 (19)	3.11	0.34
ER - ring 3	2.68 ± 0.08	0.37	2 (19)	3.12	0.33
ER - ring 4	2.64 ± 0.08	0.39	2 (19)	3.08	0.35
ER - ring 5	2.63 ± 0.09	0.40	2 (19)	3.13	0.32

4.2 Prediction of Chronological Age of Cattle

4.2.1 Prediction of age using spectra collected from muscles

As can be seen from Table 4, statistically significant models could not be developed using the striploin or eye round muscle for predicting the shear force. This was also the case when kills 1-3 were used in the phase 1 analysis. Thus, the impact of ineffective standardisation is not the main issue in this case. However, scans of eye round for prediction of shear force are worth further investigation as the results of phase 1 (ring 5. RMSECV = 5.70 Newton and R^2 = 0.58) demonstrated a better performance than the results of phase 2 (ring 5. RMSEP = 7.86 Newton and R^2 = 0.17).

Table 4. Model performance using spectra from striploin and eye round with FIR standardisation for predicting shear force (SL – Striploin and ER – Eye Round)

Spectra	ARMSEP (Newton)	R^2 Prediction	Optimum no. of LVs (no. of occur)	RMSEP Unseen (Newton)	R^2 Unseen
SL - ring 1	13.69 ± 0.40	0.03	3 (9)	11.25	0.01
SL - ring 2	13.53 ± 0.40	0.03	3 (13)	11.05	0.01
SL - ring 3	13.52 ± 0.37	0.04	3 (11)	10.91	0.03
SL - ring 4	13.29 ± 0.43	0.04	4 (11)	12.48	0.01
SL - ring 5	13.19 ± 0.35	0.04	3 (11)	11.94	0.00
ER - ring1	9.54 ± 0.26	0.08	4 (12)	8.05	0.14
ER - ring 2	9.41 ± 0.28	0.11	4 (13)	8.05	0.14
ER - ring 3	9.74 ± 0.27	0.07	4 (11)	7.91	0.16
ER - ring 4	9.62 ± 0.25	0.08	4 (15)	8.07	0.13
ER - ring 5	9.27 ± 0.24	0.12	4 (15)	7.86	0.17

4.2.2 Soluble collagen prediction using spectra collected from muscles

The results indicate (Table 5) that striploin muscle scans cannot be used to predict soluble collagen concentration which is in line with the phase 1 study which used the dataset comprising kills 1-3. The scans from eye round muscle have better predictive ability (Table 5 and Fig. 8) with scans from the muscle collected by ring 5 providing the best model performance (RMSEP = 1.46 % soluble content and R^2 = 0.41). The RMSEP is much higher than that reported in phase 1. This increase could be attributed to a combination of the use of an unseen data instead of leave-one-out cross-validation and the systematic errors introduced in kill 4 data which are not effectively removed by the FIR filter.

Table 5. Model performance using spectra from striploin and eye round with FIR standardisation for predicting soluble collage content (SL – Striploin and ER – Eye Round)

Spectra	ARMSEP	R-square	Optimum no. of LVs (no. of occur)	RMSEP Unseen	R-Square Unseen
SL - ring 1	3.60 ± 0.12	0.24	3 (10)	4.47	0.07
SL - ring 2	3.61 ± 0.14	0.23	3 (14)	4.51	0.07
SL - ring 3	3.62 ± 0.14	0.23	3 (15)	4.50	0.06
SL - ring 4	3.70 ± 0.16	0.19	3 (11)	4.37	0.10
SL - ring 5	3.85 ± 0.17	0.18	6 (7)	4.51	0.10
ER - ring 1	2.00 ± 0.10	0.44	5 (11)	1.59	0.28
ER - ring 2	2.09 ± 0.10	0.39	5 (5)	1.56	0.32
ER - ring 3	2.04 ± 0.10	0.41	5 (9)	1.57	0.31
ER - ring 4	1.91 ± 0.09	0.50	5 (11)	1.61	0.34
ER - ring 5	1.91 ± 0.08	0.49	8 (9)	1.46	0.41

Figure 8. The scatter plot of the measured vs predicted soluble collagen content using spectra of eye round muscle collected by ring 5

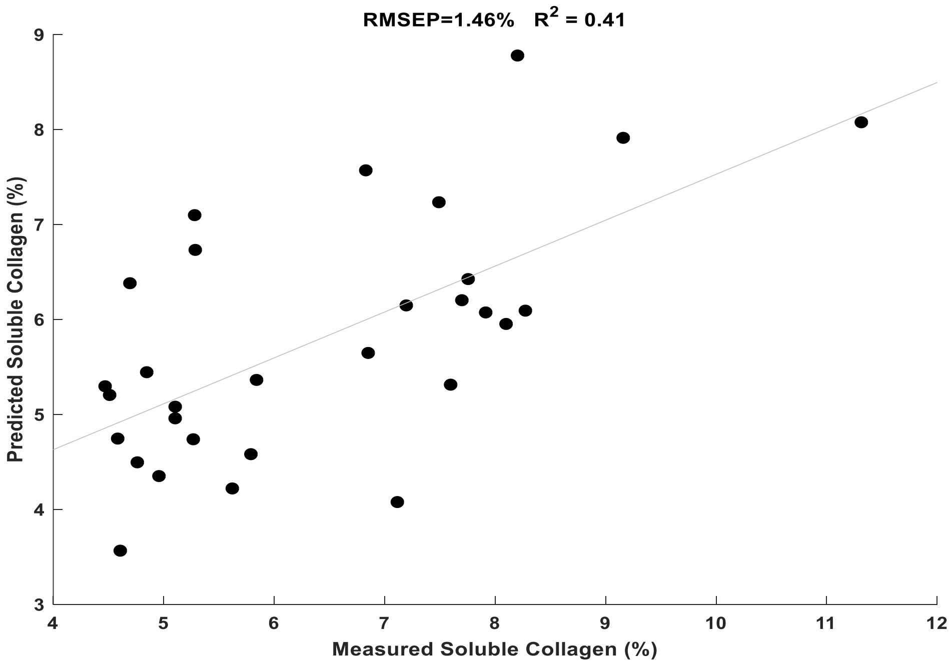

4.3 Prediction of Chronological Age Using VIS-NIR scans of live sheep

Pre-processing with SNV and automatic Whittaker filter (AWF) were considered, but were not found to improve model performance. Therefore, the results discussed here are based on mean-centred spectra and wavelength selection was not applied. It can be seen (Table 6) that spectra from the loin and neck regions could provide statistically significant models with similar model performances regardless of the source-distance or the region where the spectra were collected. The RMSEP based on the unseen dataset is consistently lower for both regions and all source-detector distances compared to the ARMSEP. As indicated in section 3.2.2, using a single unseen dataset for validation could sometimes provide a biased estimate and the true value of RMSEP may be higher than the value estimated by this random choice of unseen dataset.

Table 6. Model performance for predicting age using spectra from loin and neck region of live sheep

Spectra	ARMSEP	R^2 Prediction	Optimum LV (no. of occur)	RMSEP Unseen	R^2 Unseen
Loin - ring 1	1.50 ± 0.05	0.57	4(9)	1.15	0.70
Loin - ring 2	1.44 ± 0.05	0.60	5(11)	1.22	0.71
Loin - ring 3	1.45 ± 0.05	0.60	5(12)	1.21	0.71
Loin - ring 4	1.60 ± 0.05	0.52	4(10)	1.16	0.67
Loin - ring 5	1.70 ± 0.04	0.45	4(18)	1.19	0.64
Neck - ring 1	1.55 ± 0.06	0.50	4(20)	1.18	0.68
Neck - ring 2	1.55 ± 0.06	0.50	4(19)	1.19	0.67
Neck - ring 3	1.57 ± 0.05	0.50	4(20)	1.19	0.66
Neck - ring 4	1.61 ± 0.05	0.48	4(19)	1.18	0.65
Neck - ring 5	1.69 ± 0.05	0.45	4(18)	1.24	0.60

Another point to note is that while there is no distinct difference in performance of models based on the sampling region, an examination of Fig. 9 and 10, shows that the scatter plots using the data from the loin region have a more linear trend compared to the neck spectra. In the latter case, there is a tendency for the points to flatten out beyond about 3 years of age indicating less sensitivity to age beyond 3 years when spectra from the neck region is used. This flattening is also seen to some extent when spectra from the loin region is used. For this region, the effect is more pronounced in ring 1 (shortest source-detector distance) and rings 4 and 5 (longest source-detector distance). This suggests that the sensitivity of the model to estimate age over the full range may depend on the source-detector distance with the potential existence of an optimum source-detector distance.

Figure 9. Scatter plot of the age of sheep estimated using a PLS model with spectra collected from the loin region by rings 1-5

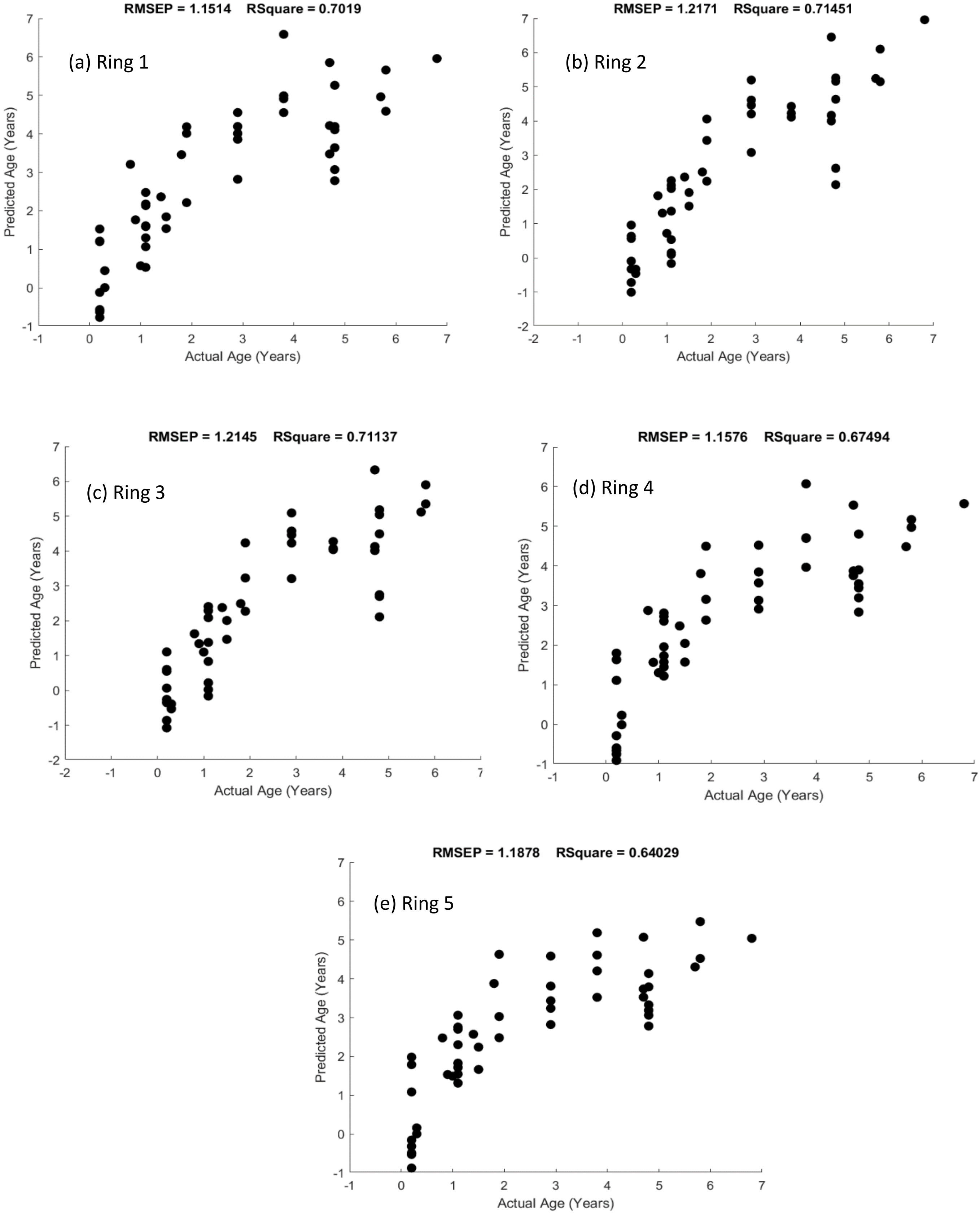

Figure 10. Scatter plot of the age of sheep estimated using a PLS model with spectra collected from the neck region by rings 1-5

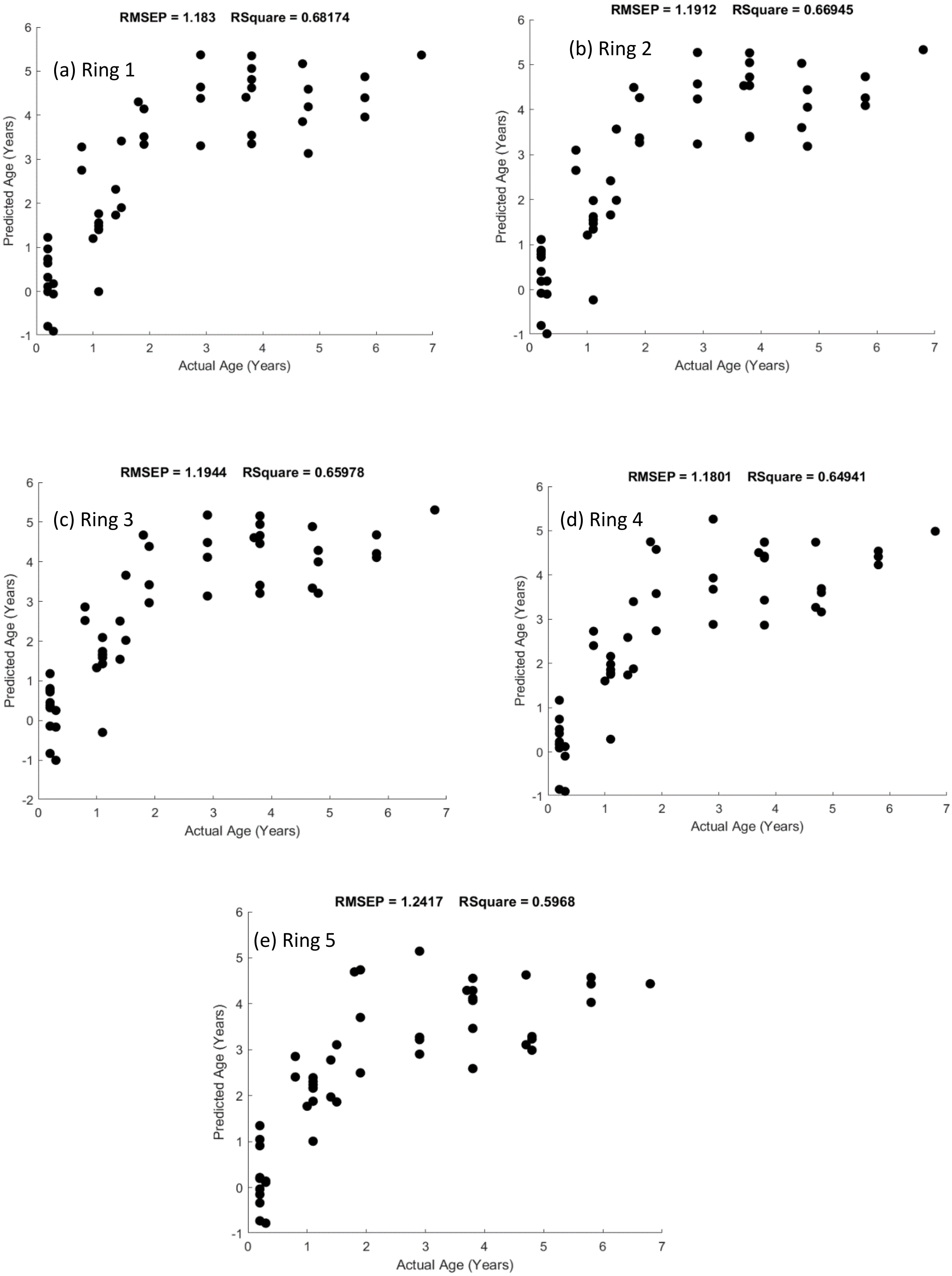

4.3.1 Stability of calibration models

Data collected from 50 animals that were scanned at 3, 6, 9 and 12 months of age was used to investigate the stability of the calibration models for estimating the age of sheep over a period of time. In this case, the calibration model built and tested using the initial dataset (scans of 208 and 207 animals acquired from the loin and neck regions respectively) was used to predict the age of the 50 selected sheep. This will provide an indication of the model stability over a 9-month period.

Table 7. Model performance over time in predicting the age of 50 sheep which were scanned at 3, 6, 9 and 12 months of age

	RMSEP (Years)				
	Test Set: 3 months old	Test Set: 6 months old	Test Set: 9 months old - Original scans	Test set: 9 months old - Wavelength shifted scans	Test Set: 12 months old
Loin - R1	0.87	1.11	5.77	1.73	1.32
Loin - R2	0.79	1.19	8.37	2.42	1.25
Loin - R3	0.83	1.22	8.35	2.53	1.40
Loin - R4	1.00	1.24	5.34	1.79	1.85
Loin - R5	1.03	1.35	3.59	1.85	1.95
Neck - R1	0.80	1.07	5.11	2.80	1.21
Neck - R2	0.85	1.14	5.22	2.90	1.36
Neck - R3	0.90	1.20	5.37	3.00	1.53
Neck - R4	0.90	1.20	4.70	2.90	1.74
Neck - R5	0.94	1.31	2.52	2.78	1.89

Examining Table 7, it can be seen that the RMSEP for the 50 animals increased slightly when the scans acquired from them were used to predict their age at 3, 6 and 12 months old. Even at 12 months old the RMSEP was still around the values indicated by the ARMSEP obtained from the RLT method and RMSEP of the unseen validation set (See Table 6). However, there was a major breakdown in the model performance in predicting the age of the animals at 9 months.

From Fig. 11, it can be seen that the scans from the sheep at 9 months indicated a significant shift in the intensity peaks compared to those from the sheep when they were 6 months old. The peaks in scans taken at 3 and 12 months line up with the peaks in scans at 6 months (not shown). This shift in peaks is due to a shift in the wavelengths caused by the instrument going out of alignment, which probably happened as a result of accidental jolting of the device during travel and shifting to the site prior to acquiring the scans. The instrument's wavelength axis was recalibrated prior to collecting the scans of the 12 months old sheep which resulted in better model performance.

In order to see if wavelength correction can be applied to the scans of 9 months old animals, dynamic time warping (DTW) technique and manual shifting of the wavelengths was tried. It was found that while manual wavelength shifting improved the results (Table 7), it was still worse than the model performance at 6 and 12 months.

The deterioration seen in model performance from going from 6 – 12 months is likely due to overall instrument drift. Thus, for the calibration model to be effective in the long-term, a rigorous protocol for instrument recalibration needs to be in place. This can be done using existing standardisation methods which require a well-defined set of calibration samples which closely mimic the optical properties of sheep tissue.

Figure 11. Scans of sheep of 6 and 9 months of age using ring 5. (a) Original scans and (b) Scans of 9 months old sheep were wavelength shifted manually

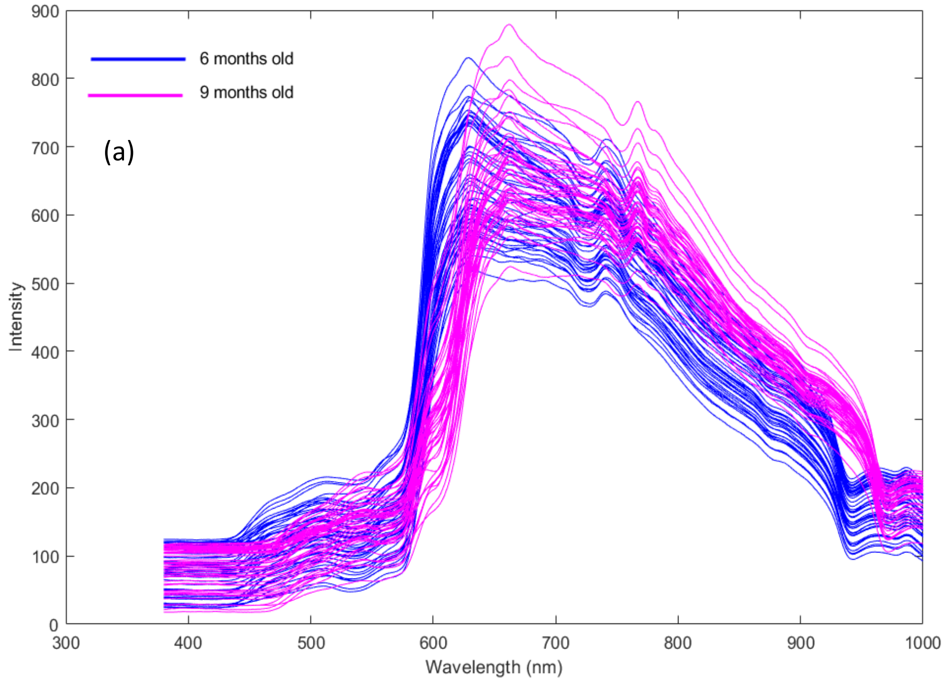

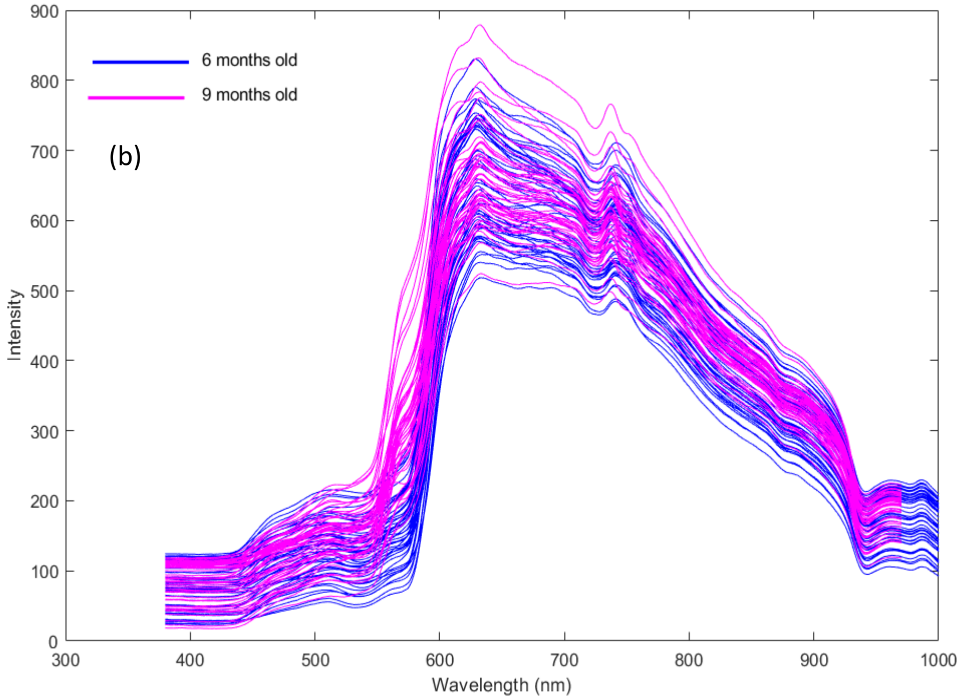

4.4 Prediction of Meat Eating Quality

An investigation of meat-eating quality using spatially resolved diffuse reflectance spectroscopy measurements was conducted using spectra collected from three different muscles from the same animals. The loin (*longissimus lumborum*), knuckle (*quadriceps femoris*) and topside (*semimembranosus*) muscles were collected and scanned using the spatially resolved diffuse reflectance Vis-NIR spectroscopy instrument at 24 post-mortem. The prediction models of the meat-eating quality were built with PLS regression using spectra collected from samples against the MSA score from consumers (testers).

4.4.1 Prediction of meat eating quality using spectra of loin muscles

The calibration models were built using spectra within the wavelength range of 500-940 nm. The spectra were mean centre before the PLS regression was undertaken. Table 8 shows model performance using spectra collected from loin muscles. Four traits of meat-eating quality were investigated using spectra from loin muscles. The results shows that there is limited potential to predict the tenderness using spectra on ring 3 with RMSEP = 6.50, R^2 = 0.44. The ability to predict the flavour varies depending on which of the 5 rings were used for measurement. Ring 1, 4, and 5 has weak ability to predict the flavour with R^2 of 0.21, 0.23, 0.23 respectively and ring 2, 3 were not able to predict the flavour. On the other hand, the juiciness and overall liking cannot be predicted using spectra in the wavelength range 500-940nm.

Further investigation using spectra from loins were conducted at wavelength range of 850 - 990nm. Andres, et al. (2007) suggest that the wavelength range 850 – 1000 nm is useful for identifying sensory eating quality traits in lamb. Therefore, Table 9 presents the model performance using spectra from the loin over the wavelength range of 850 – 990 nm.

Table 8. Model performance using spectra of loin with wavelength range 500 – 940nm for predicting meat eating quality traits

Traits	Spectra	ARMSEP	R^2 Prediction	Optimum LV (no. of occur)	RMSEP Unseen	R^2 Unseen
Tenderness						
	Loins - R1	12.25 ± 0.67	0.05	3(6)	8.11	0.13
	Loins - R2	13.77 ± 0.73	0.08	4(7)	8.26	0.06
	Loins - R3	14.57 ± 0.63	0.06	1(4)	6.50	0.44
	Loins - R4	12.57 ± 0.86	0.08	3(8)	8.05	0.10
	Loins - R5	12.50 ± 0.77	0.08	3(6)	7.99	0.06
Juiciness						
	Loins - R1	12.31 ± 0.69	0.05	3(8)	8.89	0.00
	Loins - R2	13.95 ± 0.79	0.10	3(10)	8.92	0.00
	Loins - R3	12.44 ± 0.55	0.06	3(8)	8.88	0.00

	Loins - R4	11.89 ± 0.57	0.07	3(8)	8.77	0.01
	Loins - R5	12.71 ± 0.94	0.06	3(9)	8.80	0.01
Flavour						
	Loins - R1	11.06 ± 0.74	0.19	5(8)	9.97	0.21
	Loins - R2	10.54 ± 0.63	0.10	4(8)	7.51	0.04
	Loins - R3	10.60 ± 0.77	0.14	4(6)	7.43	0.04
	Loins - R4	10.43 ± 0.88	0.10	5(9)	9.68	0.23
	Loins - R5	9.06 ± 0.42	0.27	5(9)	9.80	0.23
Overall Liking						
	Loins - R1	10.12 ± 0.43	0.19	3(14)	6.94	0.00
	Loins - R2	10.35 ± 0.62	0.14	3(15)	7.12	0.00
	Loins - R3	11.11 ± 0.60	0.11	3(10)	7.15	0.00
	Loins - R4	10.73 ± 0.69	0.14	5(10)	10.01	0.18
	Loins - R5	9.55 ± 0.50	0.16	5(11)	9.60	0.12

In Table 8, an unusual situation can be seen. The ARMSEP values in most cases are much higher than the RMSEP value obtained for the unseen validation set. A closer look at the RMSEP value for each iteration showed large variations with a few iterations exhibiting very high RMSEP values. This indicates that the model performance is highly dependent on the samples assigned to the calibration and the test set. This indicates that a dataset much larger than 50 samples is required to develop stable and precise models. This effect is also seen in Table 9.

Table 9 shows model performance for predicting meat eating quality using spectra of loin in the wavelength range of 850-990nm. Overall, the results show that spectra from loins were able to predict meat eating quality traits with some variations in model performance. Strong prediction of tenderness can be seen for rings 1, 2 and 4 with $R^2 > 0.5$. Ring 5 had a weak ability to predict the tenderness with $R^2 = 0.2$. However, there is no ability to predict tenderness using ring 3.

The model has potential to predict juiciness with the highest R^2 value among the meat-eating quality traits ($R^2 = 0.74$) on ring 5. Ring 1, 3 and 4 can predict the juiciness with the $R^2 > 0.4$. Ring 2 has no ability to predict the juiciness. Furthermore, spectra from the loin had a weak ability to predict the flavour traits with the R^2 from all rings ≤0.3 and ring 5 had no ability to predict the flavour.

The model has potential to predict the overall liking with the R^2 on ring 2, 3, and 4 is ≥0.6. Ring 1 had a weak ability to predict the overall liking. However, ring 5 had no ability to predict the overall liking where the $R^2 = 0.09$.

The results show that the wavelength range of 850-990nm for loin spectra has potential for predicting meat eating quality compared to the model prediction with wavelength range of 500-940nm. The models using the wavelength range of 850-990nm were able to predict the tenderness, juiciness, and overall liking, but it had weak ability to predict the flavour.

Table 9. Model performance using spectra from loin muscles with wavelength range of 850 – 990nm for predicting meat eating quality traits

Traits	Spectra	ARMSEP	R^2 Prediction	Optimum LV (no. of occur)	RMSEP Unseen	R^2 Unseen
Tenderness						
	Loins - R1	12.00 ± 0.96	0.10	1(11)	6.43	0.58
	Loins - R2	13.00 ± 0.96	0.12	1(10)	6.44	0.56
	Loins - R3	13.94 ± 0.87	0.34	3(8)	9.43	0.11
	Loins - R4	13.44 ± 1.13	0.21	1(15)	6.39	0.52
	Loins - R5	18.48 ± 1.40	0.20	8(9)	16.51	0.20
Juiciness						
	Loins - R1	12.94 ± 1.04	0.19	1(8)	8.55	0.46
	Loins - R2	12.87 ± 0.77	0.12	3(8)	9.64	0.02
	Loins - R3	13.56 ± 0.95	0.29	1(8)	8.55	0.44
	Loins - R4	13.54 ± 0.80	0.19	1(10)	8.48	0.47
	Loins - R5	13.40 ± 0.89	0.18	6(10)	14.98	0.74
Flavour						
	Loins - R1	10.88 ± 0.75	0.16	1(9)	6.51	0.30
	Loins - R2	11.87 ± 0.87	0.15	1(10)	6.52	0.29
	Loins - R3	11.72 ± 0.88	0.23	1(8)	6.53	0.27
	Loins - R4	11.78 ± 0.80	0.17	1(9)	6.54	0.21
	Loins - R5	13.35 ± 0.89	0.16	8(8)	11.15	0.00
Overall Liking						
	Loins - R1	12.87 ± 0.97	0.23	9(9)	7.37	0.33
	Loins - R2	11.06 ± 0.77	0.15	1(7)	6.22	0.67
	Loins - R3	11.37 ± 0.76	0.19	1(9)	6.22	0.65
	Loins - R4	10.76 ± 0.74	0.17	1(16)	6.18	0.60
	Loins - R5	14.28 ± 1.04	0.16	9(8)	15.14	0.09

4.4.2 Prediction of meat eating quality using spectra of topside muscles

Investigation of meat-eating quality were also conducted using spectra collected from topside muscle. Table 10 shows the model performance of meat-eating quality prediction using spectra from topside in the wavelength range of 500 – 940nm. The analysis for topside spectra used a similar method applied on the loin spectra. The results show that spectra from topside were able to predict eating quality traits of tenderness and juiciness. There is a strong relationship between topside spectra and juiciness traits compared to topside spectra with other traits. The highest R^2 value from the model performance is on the prediction of juiciness using spectra from ring 4 with R^2 = 0.71.
The results indicated that the flavour and overall liking cannot be predicted using spectra from topside with wavelength range of 500-940nm. Model performance of the flavour prediction shows that the R^2 value is below 0.15. Similarly, the R^2 value of the model performance of the overall liking is below 0.1 (R^2 < 0.9).
Further investigation of meat-eating quality using topside muscle was conducted using spectra with wavelength range of 850-990nm. Table 11 shows the model performance of meat-eating quality using topside muscle.

Table 10. Model performance using spectra from topside with wavelength range of 500 – 940nm for predicting meat eating quality traits

Traits	Spectra	ARMSEP	R^2 Prediction	Optimum LV (no. of occur)	RMSEP Unseen	R^2 Unseen
Tenderness						
	Topsides - R1	11.95 ± 0.58	0.18	3(14)	16.75	0.40
	Topsides - R2	13.00 ± 0.82	0.21	3(18)	16.71	0.42
	Topsides - R3	10.43 ± 0.74	0.22	3(18)	16.75	0.43
	Topsides - R4	11.37 ± 0.86	0.18	3(15)	16.52	0.37
	Topsides - R5	10.16 ± 0.71	0.26	4(11)	15.28	0.00
Juiciness						
	Topsides - R1	11.67 ± 1.12	0.25	3(14)	12.77	0.66
	Topsides - R2	10.74 ± 0.99	0.23	3(16)	12.75	0.66
	Topsides - R3	10.20 ± 1.20	0.32	3(11)	12.83	0.67
	Topsides - R4	11.21 ± 0.55	0.11	3(10)	12.81	0.71
	Topsides - R5	10.24 ± 0.58	0.18	4(11)	12.51	0.40
Flavour						
	Topsides - R1	13.04 ± 1.06	0.10	3(14)	9.84	0.12
	Topsides - R2	11.33 ± 0.76	0.07	3(17)	9.77	0.13
	Topsides - R3	13.70 ± 1.64	0.05	3(9)	9.82	0.14
	Topsides - R4	12.51 ± 0.64	0.06	3(12)	9.79	0.12
	Topsides - R5	12.36 ± 0.51	0.06	3(13)	9.87	0.02
Overall Liking						
	Topsides - R1	11.63 ± 0.83	0.11	3(12)	10.80	0.09
	Topsides - R2	11.35 ± 0.76	0.10	3(15)	10.69	0.07
	Topsides - R3	11.31 ± 0.84	0.10	3(10)	10.79	0.08
	Topsides - R4	11.81 ± 0.55	0.08	3(9)	10.75	0.08
	Topsides - R5	10.68 ± 0.53	0.08	3(11)	11.11	0.06

The results of the model performance using spectra from topside across the wavelength range of 850-990nm is presented in Table 11. Overall, the results indicated that meat eating quality traits can be predicted using topside muscles with the wavelength range of 850-990nm. The tenderness can be predicted with R^2 across ring 1, 2, 3, 4, and 5 of 0.66, 0.65, 0.65, 0.58, and 0.52 respectively. Model performance of the prediction of juiciness shows that the R^2 value on rings 1, 2, 3, 4, and 5 are 0.60, 0.60, 0.60, 0.55, 0.46 respectively.
Model performance of the flavour traits are slightly weaker compared to other traits. The R^2 of ring 2 to 5 are below R^2 = 0.4 where the highest R^2 = 0.37 was on ring 3. There is no ability to predict the flavour using spectra on ring 1 where the R^2 of ring 1 was 0.04.

The results show that the overall liking traits were able to be predicted using topside spectra with wavelength range of 850 – 990nm. The ranges of R^2 for all rings are around R^2 = 0.4 where rings 1, 2, 3, 4, and 5 are 0.48, 0.48, 0.48, 0.46, and 0.43 respectively. In comparison to model performance for predicting the overall liking traits using spectra with wavelength ranges of 500-850nm, the model performance using spectra with the wavelength range of 850-990nm were able to predict the overall liking.

Table 11. Model performance using spectra from topside with wavelength range of 850 – 990nm for predicting meat eating quality traits

Traits	Spectra	ARMSEP	R^2 Prediction	Optimum LV (no. of occur)	RMSEP Unseen	R^2 Unseen
Tenderness						
	Topsides - R1	11.64 ± 0.61	0.18	1(14)	16.00	0.66
	Topsides - R2	12.75 ± 0.88	0.27	1(8)	15.99	0.65
	Topsides - R3	13.01 ± 1.37	0.24	1(9)	15.99	0.65
	Topsides - R4	10.33 ± 0.97	0.23	1(15)	15.92	0.58
	Topsides - R5	13.39 ± 1.12	0.16	1(10)	15.70	0.52
Juiciness						
	Topsides - R1	10.20 ± 0.74	0.30	1(14)	11.87	0.60
	Topsides - R2	11.75 ± 0.92	0.33	1(7)	11.88	0.60
	Topsides - R3	11.42 ± 1.11	0.29	1(8)	11.89	0.60
	Topsides - R4	11.71 ± 0.65	0.20	1(11)	11.85	0.55
	Topsides - R5	12.42 ± 1.03	0.12	1(5)	11.72	0.46
Flavour						
	Topsides - R1	11.62 ± 0.91	0.17	3(6)	9.45	0.04
	Topsides - R2	11.75 ± 1.36	0.24	1(17)	9.42	0.36
	Topsides - R3	11.29 ± 1.02	0.24	1(10)	9.42	0.37
	Topsides - R4	15.83 ± 1.34	0.18	1(9)	9.45	0.33
	Topsides - R5	15.93 ± 0.93	0.13	1(8)	9.52	0.30
Overall Liking						
	Topsides - R1	10.87 ± 0.78	0.25	1(13)	10.06	0.48
	Topsides - R2	11.79 ± 1.12	0.35	1(12)	10.06	0.48
	Topsides - R3	11.78 ± 0.98	0.24	1(8)	10.08	0.48
	Topsides - R4	12.58 ± 0.73	0.17	1(14)	10.17	0.46
	Topsides - R5	12.31 ± 1.02	0.16	1(11)	10.29	0.43

4.4.3 Prediction of meat eating quality using spectra of knuckle muscles

The performance of the meat-eating quality prediction using spectra from knuckle muscle is presented in Table 12. The results show that there is no ability to predict the tenderness and juiciness using spectra measured from knuckle with wavelength range of 500 – 940nm. The R^2 value of the tenderness and juiciness is below 0.1. On the other hand, model performance of the flavour and overall liking show weak ability to predict the traits. The highest R^2 value of the flavour traits on ring 5 is 0.28 and the overall liking traits on ring 1 is 0.22. The results from the model performance shows the highest R^2 value using spectra from the knuckle with wavelength range of 500-850 nm is R^2 = 0.28.

Table 12. Model performance using spectra from knuckle with wavelength range of 500 – 940nm for predicting meat eating quality traits

Traits	Spectra	ARMSEP	R^2 Prediction	Optimum LV (no. of occur)	RMSEP Unseen	R^2 Unseen
Tenderness						
	Knuckle - R1	9.94 ± 0.42	0.03	3(10)	8.90	0.03
	Knuckle - R2	9.88 ± 0.50	0.05	3(8)	8.87	0.03
	Knuckle - R3	10.21 ± 0.59	0.05	3(7)	8.87	0.03
	Knuckle - R4	10.13 ± 0.40	0.05	4(5)	9.30	0.00
	Knuckle - R5	8.45 ± 0.28	0.04	3(10)	8.66	0.03
Juiciness						
	Knuckle - R1	8.36 ± 0.41	0.18	3(8)	7.47	0.02
	Knuckle - R2	9.80 ± 0.34	0.19	4(9)	7.96	0.00
	Knuckle - R3	10.16 ± 0.38	0.25	3(9)	7.43	0.02
	Knuckle - R4	10.47 ± 0.64	0.16	4(9)	8.25	0.00
	Knuckle - R5	8.94 ± 0.52	0.19	3(8)	7.53	0.04
Flavour						
	Knuckle - R1	8.20 ± 0.35	0.13	5(9)	7.43	0.25
	Knuckle - R2	8.11 ± 0.41	0.10	4(6)	7.58	0.23
	Knuckle - R3	7.54 ± 0.47	0.17	5(8)	7.61	0.21
	Knuckle - R4	8.85 ± 0.38	0.12	5(11)	7.42	0.25
	Knuckle - R5	7.89 ± 0.33	0.23	3(7)	7.42	0.28
Overall Liking						
	Knuckle - R1	7.48 ± 0.51	0.16	4(12)	6.60	0.22
	Knuckle - R2	8.79 ± 0.55	0.17	4(9)	6.63	0.21
	Knuckle - R3	9.28 ± 0.84	0.26	4(10)	6.75	0.18
	Knuckle - R4	9.02 ± 0.79	0.13	5(7)	6.82	0.16
	Knuckle - R5	7.10 ± 0.47	0.25	3(13)	6.87	0.17

Investigation of the model performance using spectra from knuckle using wavelength range of 850-990nm is presented in Table 13. The model performance using spectra from knuckle across the wavelength range of 850-990nm shows that it can only predict the overall liking trait on rings 1 and 5. The ability of prediction is weak where the R^2 on ring 1 is = 0.25 and ring 5 = 0.28. There is no ability to predict the tenderness, juiciness and flavour traits using spectra from knuckle with wavelength range of 850-990nm.

Table 13. Model performance using spectra from knuckle with wavelength range of 850 – 990nm for predicting meat eating quality traits

Traits	Spectra	ARMSEP	R^2 Prediction	Optimum LV (no. of occur)	RMSEP Unseen	R^2 Unseen
Tenderness						
	Knuckle - R1	8.40 ± 0.53	0.21	3(7)	9.41	0.01
	Knuckle - R2	10.55 ± 0.75	0.14	3(9)	9.35	0.01
	Knuckle - R3	9.23 ± 0.56	0.15	3(12)	9.55	0.00
	Knuckle - R4	9.66 ± 0.60	0.17	3(7)	9.08	0.05
	Knuckle - R5	8.96 ± 0.53	0.22	1(8)	9.14	0.00
Juiciness						
	Knuckle - R1	6.33 ± 0.42	0.36	9(6)	11.96	0.06
	Knuckle - R2	8.44 ± 0.59	0.16	3(5)	7.52	0.05
	Knuckle - R3	9.76 ± 0.72	0.29	3(6)	8.63	0.00
	Knuckle - R4	8.87 ± 0.40	0.16	1(9)	7.84	0.00
	Knuckle - R5	9.36 ± 0.98	0.26	3(8)	8.06	0.12
Flavour						
	Knuckle - R1	7.25 ± 0.61	0.21	1(8)	8.53	0.04
	Knuckle - R2	8.92 ± 0.59	0.20	7(6)	9.72	0.01
	Knuckle - R3	9.07 ± 0.51	0.22	1(11)	8.53	0.04
	Knuckle - R4	7.99 ± 0.80	0.18	1(14)	8.59	0.04
	Knuckle - R5	7.83 ± 0.57	0.17	1(11)	8.64	0.04
Overall Liking						
	Knuckle - R1	6.72 ± 0.36	0.28	9(8)	8.29	0.25
	Knuckle - R2	7.26 ± 0.54	0.20	7(9)	8.26	0.05
	Knuckle - R3	7.96 ± 0.36	0.23	1(7)	7.66	0.00
	Knuckle - R4	7.77 ± 0.68	0.21	1(10)	7.77	0.00
	Knuckle - R5	7.68 ± 0.44	0.25	3(8)	6.82	0.28

5. Conclusion

One aspect of this study was aimed at validating the initial results of phase 1 study which was focussed on estimating the chronological age of cattle using VIS-NIR spectroscopy measurements of hide and that study was limited by the distribution of age in the cows on which data was collected. So, in phase 2, data were collected from an additional 93 cows so that a substantial dataset was available for testing the feasibility of estimating age of cattle using Vis-NIR spectroscopy. Significant challenges were encountered in collecting a suitable dataset that covered a sufficiently evenly distributed cattle age over the age range of interest. As a result of this and considering the time gap between phase 1 and phase 2 studies, the entire data collection was spread over 2 years. This was a challenge which was not expected at the beginning of the phase 1 of the project.

As a result, systematic differences between datasets collected from phase 1 and phase 2 were observed. This had an adverse effect on model performance. A standardisation procedure using the finite impulse response (FIR) filter was used to correct the systematic variations arising from changes in instrument characteristics over time. This was found to have a limited impact in decreasing the prediction error with the best model that could be produced having an RMSEP of 2.71 years and R^2 of 0.4. The results, while indicating a weak correlation of hide spectra with cattle age, are not sufficient in terms of its usefulness in practice unless the degradation in model performance due to systematic instrument variations can be removed. Furthermore, the complexity of the protocol due to the nature of collecting the hide samples and making it measurement ready, made it difficult to achieve consistently accurate measurements. This could have also contributed to the high prediction errors. Our later experience with devising the experimental protocol and collecting spectra from live sheep, indicates that using live animals will be less complicated than collecting spectra at the abattoir during slaughters.

Therefore, three recommendations arise from the study for determining cattle age. Firstly, the collection of calibration dataset should be over a short time span of 2 – 3 months. This number is based on typical calibration dataset collection times encountered in a variety of applications which are usually much shorter than 3 months. Secondly, given this may not be feasible a rigorous protocol for standardising the instrument must be developed. In fact, this would be required for long-term maintenance of the calibration model since the device will be used for a long time and carrying out a full calibration at regular intervals would not be feasible. This will entail collecting spectra from a carefully chosen set of samples made of material whose spectra has similar characteristics as those of the cattle hide tissue. One approach would be to develop "tissue phantoms" i.e. simulated tissue, similar to the ones used in the field of tissue optics. Thirdly, given the experience during data collection from live sheep, acquiring spectra from live cattle instead of hides at slaughter will be preferable. In this case, the challenges in getting access to an adequate number of live cattle evenly spanning the desired age range would have to be addressed.

It was found that the Vis-NIR measurements in the wavelength range considered here cannot be used to predict shear force using spectra collected from striploin muscle with an R^2 of less than 0.05. However, the prediction of shear force using scans of muscles with a higher content of connective tissue such as eye round muscle is worth of further investigation.
Despite the systematic instrument variations affecting the models, results suggest that soluble collagen content can be predicted using spectra from eye round with the best model having an RMSEP of 1.46% and R^2 of 0.41. On the other hand, spectra from striploin muscles had negligible correlation to soluble collagen content the models having an R^2 of less than 0.1.

The study indicates that the age of sheep can be estimated using spectra collected from the loin and neck region of live animals (Loin: Ring 1, RMSEP = 1.15 years, R^2 = 0.68; Neck: Ring 1, RMSEP = 1.18,

R^2 = 0.68). While there was no distinct difference in performance of models based on the sampling region, the model based on spectra from the neck appeared to be less sensitive to age beyond about 3 years. This flattening is also seen to some extent when spectra from the loin region is used. For this region, the effect more pronounced in ring 1 (shortest source-detector distance) and rings 4 and 5 (longest source-detector distance). This suggests that the sensitivity of the model to estimate age over the full range may depend on the source-detector distance with the potential existence of an optimum source-detector distance.

The stability of the calibration models for predicting the age of sheep was studied by collecting spectra from a batch of 50 sheep when they were 3, 6, and 9 months old. A slight deterioration in model performance over time can be observed compared to the initial estimates of prediction error given above (At 12 months, Loin: Ring 1, RMSEP = 1.32 years, Neck: Ring 1, RMSEP = 1.21). As in the case of the cattle data, changes in device characteristics due to drift, parts replacement, or misalignment, will affect the long-term usability of the calibration models. Therefore, an instrument recalibration and standardisation protocol has to be developed and applied to the instrument prior to data collection.

The investigation of the meat-eating quality using spatially resolved diffuse reflectance spectroscopy instrument shows spectra with wavelength range of 500-940nm has some limitation in predicting the meat-eating quality traits, whereas narrowing the wavelength ranged the wavelength range to 850-990nm resulted in models with better prediction of the meat-eating quality traits. Overall, spectra from loin and topside muscles have limited potential to predict the meat-eating quality traits. The results show that the topside muscle has highest R^2 value for predicting tenderness (R^2 = 0.66, RMSEP=16) and flavour (R^2 = 0.37, RMSEP = 9.42) compared to other muscles. The highest R^2 value for predicting juiciness was from the model performance using loin spectra (R^2 = 0.74, RMSEP = 14.98). On the other hand, spectra from knuckle muscle had weak ability to predict the meat-eating quality traits. The results suggest that meat eating quality traits can be predicted with limited ability using spectroscopy in the wavelength range of 850-990nm. The large uncertainty in the predictions could be addressed by collecting a much larger dataset.

6. Acknowledgements

We would like to thank Dr. Geert Geesink for assisting with project design and meat science input; Dr. Linda Cafe (NSW DPI Livestock Industries Centre), Mr. Matias Suarez (NSW DPI), Mr. Jason Siddell (NSW DPI) and Mr. Christian Duff (Angus Australia) for providing animal background information; Dr. Peter McGilchrist (UNE), Mrs. Xuemei Han (UNE), Mr. Aaron van den Heuvel (UNE), Mr. Michael Raue (UNE), Mr. Cameron Steel (UNE), Mr. Giancarlo M. Souza (UNE, USP – Universidade de São Paulo – Brazil), Mr. Maxwell Newsome (LLS, Inverell), Ms. Katie Austin (NSW DPI), Mrs. Kylie Cooley (NSW DPI), Ms. Laura Penrose (NSW DPI), Mr. Alistair Donaldson (NSW DPI), Dr. Steph Fowler (NSW DPI) and Dr. Douglas Guimaraes (NSW DPI, Cowra/Universidade Federal de Lavras – Brazil) for assistance with beef abattoir data collection; NSW Department of Primary Industries Mrs. Edwina Toohey and Mr. Jason Siddell for liaising with meat processors; NSW Department of Primary Industries Ms. Laura Penrose, Mrs. Serey Woodgate, Mr. Reg Woodgate, Mr. Gustavo Santos, Ms. Hanna Buckley, Mr. Daichi Nishino and University of New England Dr Peter McGilchrist, Mrs. Xuemei Han and Ms. Ella Palmer for assistance with meat analysis; MSA's Miss Jessira Perovic and Mrs Janine Lau for their grading of our beef carcases; NSW Department of Primary Industries Mr. Phil Goodacre, Mr. George Carney, Dr. Gordon Refshauge, Mrs. Kylie Cooley and Mr. David Cupitt for assistance with live sheep data collection, Dr Sue Mortimer for allowing her access to the samples.

7. References

Adamovsky G., Sotomayor J. L., Krasowski M. J., Eustace J. G., 1990, *Compensation for effects of ambient temperature on rare-earth doped fiber optic thermometer*, Proc. SPIE 1169, Fiber Optic and Laser Sensors VII, (13 February 1990); https://doi.org/10.1117/12. 963071.

Andres S., Murray I., Navajas E. A., Fisher A. V., Lambe N. R., & Bunger L.,2007, *Prediction of sensory characteristics of lamb meat samples by near infrared reflectance spectroscopy, Meat Sci, 76*(3), 509-516. doi:10.1016/j.meatsci.2007.01.011

Bonny, S.P.F., Pethick, D.W., Legrand, I., Wierzbicki, J., Allen, P., Farmer, L.J., Polkinghorne, R.J., Hocquette, J.-F., Gardner, G. E., 2016. *Ossification score is a better indicator of maturity related changes in eating quality than animal age*. Animal, 10, 718–72.

Bouveresse E., & Massart D.L., 1996, *Standardisation of near-infrared spectrometric instruments: A review*, Vibrational Spectroscopy, 11(1), pp. 3-5, doi: 10.1016/0924-2031(95)00055-0.

Cafe, L.M., McIntyre, B.L., Robinson, D.L., Geesink, G.H., Barendse, W., Greenwood, P.L., 2010, *Production and processing studies on calpain-system gene markers for tenderness in Brahman cattle: 1. Growth, efficiency, temperament, and carcass characteristics*. Journal of Animal Science, 88, 3047–3058.

Duarte, M.S., Paulino, P.V.R., Fonseca, M.A., Diniz, L.L., Cavali, J., Serão, N.V.L., Gomide, L.A.M., Reis, S.F., Cox, R.B., 2011, *Influence of dental carcass maturity on carcass traits and meat quality of Nellore bulls*. Meat Science, 88, 441–446.

Fearn T.,2001, *Standardisation and calibration transfer for near infrared instruments: A Review*, Journal of Near Infrared Spectroscopy, 9(4), pp. 229–244, doi: 10.1255/jnirs.309.

Hjalmarsson, P., and Thennadil, S. N., 2008, *Determination of glucose concentration in tissue-like material using spatially resolved steady-state diffuse reflectance spectroscopy*. Proceedings of SPIE. Complex dynamics and fluctuations in biomedical photonics V, Valery V. Tuchin, Lihong V. Wang (Eds.) vol. 6855, paper 685508.

Hopkins, D. L., Stanley, D. F., Martin, L. C. & Gilmour, A. R., 2007, *Genotype and age effects on sheep meat production. 1. Production and growth*. Australian Journal of Experimental Agriculture, 47 (10), 1119-1127.

Lawrence, T.E., Whatley, J.D., Montgomery, T.H., Perino, L.J., 2001, *A comparison of the USDA ossification-based maturity system to a system based on dentition*. Journal of Animal Science, 79, 1683–1690.

Mark H., and Jerome Workman Jr., 2017, *Bias and slope correction*, Spectroscopy, 32(2), pp. 24-30, 01 Feb 2017

MATLAB version 9.1.0.441655. Natick, Massachusetts: The Mathworks Inc., 2016.

MSA beef information kit, 2018, Meat & Livestock Australia Limited, https://www.mla.com.au/ globalassets/mla-corporate/marketing-beef-and-lamb/documents /meat-standards-australia/msa-beef-tt_full-info-kit-lr.pdf

Palendeng M., Alvarenga T.I.R.C., Fowler S., Hopkins D.L., McGilchrist P., Thennadil S.N., 2020, *Estimation of Chronological Age of Cattle Using Spatially Resolved Diffuse Reflectance Measurements of Hide,* IEEE Sensors Journal,20(15):8673-82.

PLS_Toolbox 8.2.1, 2016, Eigenvector Research, Inc., Manson, WA USA 98831, software available at http://www.eigenvector.com.

Prieto, N., Juárez, M., Dugan, M.E.R., ZIjlstra, R.T., Aalhus, J.L., 2015, *Near infrared spectroscopy on ears to classify pigs based on carcass and fat composition*. Meat Science, 112.

Raines, C.R., Dikeman, M.E., Unruh, J.A., Hunt, M.C., Knock, R.C., 2008, *Predicting cattle age from eye lens weight and nitrogen content, dentition, and United States Department of Agriculture maturity score*. Journal of Animal Science, 86, 3557–3567.

Ruchti, T.L., Thennadil, S., Malin, S.F., Rennert, J., 2002, *System for the noninvasive estimation of relative age*. US Patent No 6,501,982 B1.

Salim G. R., Fox N. P., Theocharous E., Tong Sun, Grattan K. T. V., 2011, *Temperature and nonlinearity corrections for a photodiode array spectrometer used in the field Saber*, Applied Optics, 50 (6), pp. 866-875, 20 February 2011.

Schönfeldt, H.C., Strydom, P.E., 2011, *Effect of age and cut on tenderness of South African beef*. Meat Science, 87, 206–218.

Thennadil S., Palendeng M., Alvarenga T., Fowler S., Hopkins D., 2019, *Estimation of the age/maturity of beef and sheep using spatially resolved visible near infrared spectroscopy - Final Report L.EQT.1626*, MLA, https://www.mla.com.au/research-and-development/search-rd-reports/final-report-details/Estimation-of-the-age-maturity-of-beef-and-sheep-using-spatially-resolved-visible-near-infrared-spectroscopy/4145.